

BENCHMARKING OF SYNTHESIZED 3-D S_N TRANSPORT METHODS FOR PRESSURE VESSEL FLUENCE CALCULATIONS WITH MONTE CARLO

J.C. Wagner, A. Haghghat, B.G. Petrovic, and H.L. Hanshaw
Nuclear Engineering Department
The Pennsylvania State University
University Park, PA 16802
(814) 865-1341

ABSTRACT

Monte Carlo calculations of pressure vessel (PV) neutron fluence have been performed to benchmark discrete ordinates (S_N) transport methods. These calculations, along with measured data at the ex-vessel cavity dosimeter, provide a means to examine various uncertainties associated with the S_N transport calculations. For the purpose of the PV fluence calculations, synthesized 3-D deterministic models are shown to produce results that are quite comparable to results from Monte Carlo methods, provided the two methods utilize the same multigroup cross section libraries. Differences between continuous energy Monte Carlo and multigroup S_N calculations are analyzed and discussed.

I. INTRODUCTION

As many commercial nuclear light water reactors (LWR) approach the end of their design lifetime, it is of great consequence that reactor operators/owners and regulators be able to accurately characterize the structural integrity of the reactor pressure vessel (RPV). The assurance of RPV integrity is important for financial reasons, as well as safety reasons, due to the possibility of plant life extensions. The structural integrity of the RPV is degraded by the bombardment of high-energy neutrons, and thus, in order to qualify the integrity, the neutron fluence at the RPV must be well known. To this end, the S_N transport method¹ is used to determine a synthesized 3-D flux distribution based on 1-D and 2-D transport calculations.² In the past, these calculations have been benchmarked based on measured data at relatively few locations corresponding to the ex-vessel cavity dosimeters and/or the in-vessel capsules. In addition, the S_N calculations contain uncertainties associated with multigroup libraries, multi-dimensionality, geometric approximations, and angular discretization. In order to determine the RPV neutron fluence as accurately as possible, it is necessary to understand the effect(s) of these uncertainties. The Monte Carlo method offers explicit geometric representation and continuous energy and angular simulations, and thus, is well suited for benchmarking the S_N transport calculations.

This paper compares results from Monte Carlo and S_N transport calculations for Three Mile Island unit 1 (TMI-1) cycle 7. In addition, comparisons are made between calculated reaction rates and experimental data at the cavity dosimeter. The Monte Carlo results are considered the reference from which the deterministic results will be evaluated. Differences between the results are analyzed, and attempts at their qualification are made.

II. METHODS USED

For the discrete ordinates S_N calculations, the DORT code³ was used to simulate R- θ , R-Z, and R reactor models. The resultant flux distributions were synthesized to obtain an equivalent R- θ -Z flux distribution. For these calculations, the SAILOR 47-group cross-section library⁴ and a symmetric S_8 quadrature set with convergence criterion of 0.01% were used.

One of the difficulties associated with deterministic methods is the geometric approximations that must be made when modeling reactor systems. Figure 1 shows one octant of the DORT model for TMI-1 and demonstrates some of the geometric approximations necessary for this application; specifically, the use of jagged arcs to describe the rectangular fuel assemblies and the cylindrical cavity dosimeter.

For the Monte Carlo calculations, the MCNP4A code⁵ was used. Figure 2 shows one octant of the MCNP model that represents one octant of the TMI-1 reactor, from the core through the concrete wall. This model explicitly represents the rectangular and cylindrical regions in three dimensions, while the deterministic model uses cylindrical geometries to represent rectangular regions in only two dimensions. For the axial dimension, both models extend from the bottom of the lower grid plate to the top of the upper grid plate. The reflective boundary condition is used for the left, front, and back surfaces, and a vacuum boundary condition is prescribed on the top, bottom, and right surfaces.

Unless stated otherwise, MCNP utilizes a continuous form of the ENDF/B-V cross-section library, while DORT employs a multigroup version of ENDF/B-IV that has been prepared for this type of analysis (i.e., SAILOR). The source distributions for both models were prepared based on the TMI-1 cycle 7 pinwise power and burnup distributions and an equivalent fission spectrum for U and Pu fissile isotopes⁶. In MCNP, this distribution is represented by a probability distribution function at 24 axial locations in each fuel pin of the last two (peripheral) layers of assemblies. The motivations for considering only the peripheral assemblies are: (1) the negligible contribution of the source neutrons from the inner assemblies to the ex-vessel cavity dosimeter⁷ and (2) the large volume of data.

III. DISCUSSION OF RESULTS

A. MCNP and DORT Comparisons

As mentioned, the purpose of this work is to thoroughly compare Monte Carlo and S_N results and to quantify uncertainties associated with the S_N calculations that do not exist in continuous energy Monte Carlo calculations. In this section we compare the two techniques by comparing neutron energy and spatial distributions throughout the reactor models. Specifically, radial, axial, and azimuthal neutron flux distributions, neutron spectra, and reaction rates at the ex-vessel cavity dosimeter are compared.

Figure 3 compares radial group flux distributions at the core midplane and 30° azimuth extending from the core periphery to the cavity dosimeter. The error bars on the MCNP results correspond to 1σ statistical uncertainties and are within 5%. The energy groups to which the group fluxes are referenced are consistent with the SAILOR 47-group structure. For this application we are interested in energies above 1.0 MeV (i.e., groups 1 through 19).

As the neutrons travel outward in the radial direction from the core periphery (170 cm), they encounter the core barrel (179-184 cm), the thermal shield (187-192 cm), the RPV (217-239 cm), the cavity region (239-350 cm), and finally the cavity dosimeter (350 cm). The behavior of the group fluxes with respect to the different material regions follows our expectations, and the flux distributions as calculated by MCNP and DORT are shown to be quite similar. For the most part, the differences are negligible at the core periphery, increasing through the core barrel and thermal shield, remaining relatively constant within the downcomer, increasing through the RPV, and then remaining relatively constant beyond the RPV. DORT predicts less neutron transmission through stainless steel than MCNP. Also, the relative differences beyond the RPV are significantly larger (~30%) for the lower energy groups than for the higher energy groups (~20%).

In order to compare as many points as possible and subsequently properly evaluate the S_N results, we compare the MCNP and DORT results in the axial and azimuthal directions as well. Although the deterministic model is not truly three-dimensional, insight into the appropriateness of the synthesis technique can be obtained by such a comparison. Figure 4 compares axial ($\sim \pm 180$ cm from the core midplane) flux distributions, as calculated by DORT and MCNP, corresponding to the $\frac{3}{4}T$ position of the RPV and 30° azimuth. This figure demonstrates that DORT is able to predict similar shapes to those predicted by MCNP, and that DORT predicts a fewer number of neutrons at the $\frac{3}{4}T$ position of the RPV throughout the axial direction. It is important to note that no significant trends in the differences are apparent. The fact that the MCNP flux distribution do not exhibit smooth behavior like the DORT flux distributions is expected and can be directly attributed to the methods (i.e., Monte Carlo calculated fluxes (tallies) at adjacent locations are not directly dependent on each other, while deterministically calculated fluxes are).

Figure 5 compares azimuthal flux distributions at the core midplane and $\frac{3}{4}T$ position of the RPV. Examination of this figure leads to the same conclusions that were stated for the axial flux distributions; namely, the flux distributions are similar and DORT predicts lower fluxes than MCNP.

For determination of material damage, it is necessary to accurately calculate the neutron spectra at various locations within the RPV. Figure 6 shows the neutron spectra corresponding to the core midplane and 30° azimuth for the $\frac{3}{4}T$ and $\frac{1}{2}T$ positions of the RPV. This figure reveals discrepancies between the DORT and MCNP results

within 20% for all but the first group, which is plagued by differences of ~50%. The neutron behavior described by these two figures is consistent with that revealed in the analysis of radial flux distributions; namely, the agreement between DORT and MCNP deteriorates within the RPV.

Models used for the RPV neutron fluence calculations generally rely on measured reaction rates for benchmarking purposes. For TMI-1, measured data exist for the $^{63}\text{Cu}(n,\alpha)$, $^{54}\text{Fe}(n,p)$, and $^{58}\text{Ni}(n,p)$ reactions, which have threshold energies of ~4.97, 1.0, and 1.0 MeV, respectively. Table I lists ratios of calculated-to-experimental (C/E) reaction rates corresponding to the MCNP and DORT results. The SAILOR response cross sections were used for both calculations. The ratios calculated by DORT are all approximately 15% lower than those calculated by MCNP. Also, both DORT and MCNP underpredict all three of the reaction rates due to the use of pre-ENDF/B-VI cross sections in this analysis^{8,9}.

Table I. Reaction Rates at Cavity Dosimeter for TMI-1

Reaction	DORT	MCNP ^a	Relative Difference(%) ^b
$^{63}\text{Cu}(n,\alpha)$	0.780	0.894 (.018)	-12.8
$^{54}\text{Fe}(n,p)$	0.813	0.949 (.016)	-14.3
$^{58}\text{Ni}(n,p)$	0.789	0.936 (.015)	-15.7

^a Numbers in parenthesis are 1σ uncertainties

^b [(DORT - MCNP) / MCNP]

Since the cavity dosimeter is located near the core midplane, we believe the effect of geometric approximations in the deterministic model (i.e., approximations in modeling and 3-D synthesis) are negligible. Also, a recent study of the effect of quadrature order¹⁰ indicates that the use of a S_8 quadrature order is adequate (within a few percent) for the RPV fluence calculations (i.e., the "ray-effect" is relatively negligible). Therefore, we expect the major portion of the discrepancies to be associated with the multigroup cross sections.

B. Multigroup MCNP and DORT Comparisons

In order to determine the effect of the multigroup cross sections, an MCNP calculation has been performed with the SAILOR multigroup library (the SAILOR library was processed into a form suitable to MCNP with the CRSRD code¹¹). Figure 7 compares radial group flux distributions, and demonstrate good agreement between DORT and MCNP when both codes use the same cross-section data. In all cases, the relative differences between MCNP and DORT are less than ~10%; as opposed to ~40% for continuous energy MCNP. The fact that the MCNP results are slightly higher is to be expected and can be attributed to the fact that although MCNP is using the same angular data as DORT, it is using it differently. (The MCNP simulation is continuous in the angular treatment while DORT is discrete.)

As further testimonial to the good agreement, we revisit the neutron spectra at the $\frac{1}{4}T$ and $\frac{1}{2}T$ positions of the RPV in Figures 8 and 9. These figures demonstrate excellent agreement (within 10%) between MCNP and DORT when both use the SAILOR cross sections, and that the majority of the discrepancies observed in the reference comparisons can be attributed to the cross sections.

Further support for this assertion is presented in Table II, which compares C/E ratios. The last two columns show the relative differences between DORT and MCNP when both codes use the SAILOR multigroup library, and when MCNP uses the continuous energy ENDF/B-V library, respectively. It appears that the maximum difference is reduced by ~10% when the two codes use the same cross sections. In addition, the small differences between DORT and MCNP can be attributed to a combination of MCNP's continuous angular treatment and statistics.

TABLE II. Effect of Multigroup Cross Sections on Reaction Rates

Reaction	MCNP (C/E) ^a		Relative Difference(%) ^b	
	SAILOR	ENDF/B-V	DORT from MCNP with SAILOR	DORT from MCNP with ENDF/B-V
⁶³ Cu(n,α)	0.788(0.057)	0.894(0.018)	-1.0	-12.7
⁵⁴ Fe(n,p)	0.873(0.046)	0.949(0.016)	-6.9	-14.3
⁵⁸ Ni(n,p)	0.854(0.041)	0.936(0.015)	-7.6	-15.7

^a Numbers in parenthesis are 1σ uncertainties

^b [(DORT - MCNP) / MCNP]

C. Multigroup Cross Sections

At this point, it may be concluded that the flux distributions and cavity dosimeter activities predicted via the 3-D synthesis multigroup S_N transport calculations are within 10% of the multigroup MCNP results. While these calculations clearly demonstrate the effect of the multigroup libraries, they do not, however, conclusively reveal the origin of the effect (i.e., P_3 truncation, group structure, self-shielding effect, or some combination of the three). Therefore, we investigate the effect of these approximations.

One possible explanation for the aforementioned results is that the order of the Legendre polynomial expansion (P_3) is insufficient to properly approximate the anisotropy present in the differential scattering cross sections. In other words, the P_3 truncation may not be able to accurately represent the forward-peaked behavior of the high energy neutrons that are being simulated.

The BUGLE-93 library¹² contains Legendre order P_7 , and is thus, well suited for examining the effect of the Legendre expansion truncation. The CRSRD code was used to create four libraries from BUGLE-93 suitable to MCNP. These libraries differed in the number of expansion terms used, which were P_1 , P_3 , P_5 , and P_7 . Using these four libraries, full MCNP calculations were performed, and the results are listed in Table III in the form of C/E ratios. The last three columns of Table III list relative differences for the P_1 , P_3 , and P_5 data with respect to the P_7 data, and clearly demonstrate the effect of the truncation. The P_1 data significantly underpredict (~10%) the P_7 solution, while the P_3 data slightly overpredict (~4%) the P_7 solution. The P_5 data, on the other hand, very nearly predict (within the 1σ statistical uncertainties) the solution calculated with P_7 data.

TABLE III. Effect of Legendre Expansion Truncation on Reaction Rates

Reaction	MCNP ^a with BUGLE-93 (C/E)				Relative Difference(%) ^b		
	P_1	P_3	P_5	P_7	P_1 from P_7	P_3 from P_7	P_5 from P_7
⁶³ Cu(n,α)	0.798	0.936	0.884	0.901	-11.4	3.8	-1.9
⁵⁴ Fe(n,p)	0.936	1.140	1.084	1.094	-14.4	4.2	-0.9
⁵⁸ Ni(n,p)	0.908	1.096	1.040	1.055	-14.0	3.8	-1.5

^a All 1σ uncertainties are between two and three percent

^b "A from B" should be interpreted as [(A - B) / B]

Since we have found the effect of the Legendre expansion truncation to be essentially negligible and a previous study related to the effect of self-shielding in the multigroup constants¹³ has shown negligible effects for

energies greater than 1.0 MeV, we turn our attention to the group structure. The energy group structure of any multigroup library is extremely important, and must be selected in such a way that the energy dependence of the cross section data for all materials in the library be properly represented.

In order to determine whether or not the SAILOR group structure is adequate for this application, we must compare the group-wise data to continuous energy data and perform calculations with a fine-group library. To facilitate this comparison, two new multigroup libraries were created from the VITAMIN-C fine-group library.¹⁴ The first of these two employs the VITAMIN-C 171 group structure (with energy self-shielding), while the second employs the SAILOR 47 group structure. The latter library was created in order to avoid any inconsistencies/differences in the basic data and/or self-shielding calculations; a detailed discussion is provided in Ref. 13. Herein, these two libraries will be referred to as the 171grp and 47grp libraries, respectively.

Before performing calculations, it is instructive to compare iron cross sections from the three aforementioned libraries. Figure 10 compares the total cross section for iron from the continuous energy ENDF/B-V, 171grp and 47grp libraries. This figure shows the complicated behavior of the cross section data, and demonstrates that the energy groups in the 47-group structure are rather broad in the energy range above 3 MeV. In addition, the 171grp library exhibits much better agreement with respect to the continuous energy data.

To quantify the differences, MCNP calculations were performed with both the 47grp and 171grp libraries. Table IV compares C/E ratios calculated by MCNP with the 47grp, 171grp, and continuous energy ENDF/B-V libraries. Examination of this table reveals that the C/E ratios calculated by MCNP with the 171grp library are ~6% higher than those calculated by MCNP with the 47grp library. In addition, the last two columns provide further evidence that the 171grp library calculations more closely agree to the continuous energy calculations. The 171grp results are compared to the 47grp results, and not to the MCNP results using the SAILOR library for consistency.

TABLE IV. Effect of Group Structure on Reaction Rates

Reaction	MCNP (C/E) ^a		Relative Difference(%) ^b	
	47grp	171grp	ENDF/B-V from 47grp	ENDF/B-V from 171grp
⁶³ Cu(n,α)	0.852(0.030)	0.907(0.025)	4.9	-1.4
⁵⁴ Fe(n,p)	0.821(0.020)	0.877(0.016)	15.6	8.2
⁵⁸ Ni(n,p)	0.845(0.022)	0.907(0.018)	10.8	3.2

^a Numbers in parenthesis are 1σ uncertainties

^b "A from B" should be interpreted as [(A - B) / B]

V. CONCLUSIONS

From this calculational/experimental benchmark study, we can conclude that the synthesized 3-D deterministic transport methods are satisfactory for the RPV fluence calculations. The S_N transport methods predict fewer (~15-20%) high energy neutrons in the RPV than continuous energy Monte Carlo methods, while the flux distributions and cavity dosimeter activities predicted via multigroup S_N transport calculations are within 10% of the multigroup MCNP results. Uncertainties associated with S_N transport such as geometric approximations and multi-dimensionality effects are negligible, while approximations associated with multigroup libraries and angular treatments are notable. A large portion of the differences between the continuous energy and multigroup results can be attributed to the energy group structure, while the differences due to the Legendre order truncation are relatively insignificant. Also, the differences between multigroup Monte Carlo and multigroup S_N methods can be mostly attributed to the respective angular treatments and statistics.

If one so desired, biasing factors based on the ratio of the continuous energy Monte Carlo and multigroup S_N calculations could be developed and used to *correct* existing multigroup S_N results. These biasing factors would necessarily account for the inability of the multigroup structure to properly simulate particle energy transfer.

Future work will involve the determination of the optimum number of energy groups required to reproduce

the continuous energy Monte Carlo results with the multigroup S_N , within the statistical uncertainties, and the subsequent creation of an *effective* broad group library for pressure vessel fluence calculations.

ACKNOWLEDGEMENTS

The authors would like to acknowledge the financial support provided by the GPU Nuclear Corporation, and the equipment grant (two IBM RISC/6000 workstations) by the IBM Corporation.

REFERENCES

1. E.E. Lewis, W.F. Miller, *Computational Methods of Neutron Transport*, John Wiley & Sons, New York (1984).
2. R.E. Maerker, "LEPRICON Analysis of Pressure Vessel Surveillance Dosimetry Inserted into H. B. Robinson-2 During Cycle 9," *Nucl. Sci. Eng.*, **96**, 263-289 (1987).
3. W.A. Rhoades and R.L. Childs, "The DORT Two-Dimensional Discrete Ordinates Transport Code System," RSIC-CCC-484, ORNL Radiation Shielding Information Center, Oak Ridge, TN (1989).
4. G.L. Simmons and R. Roussin, "SAILOR - A Coupled Cross-Section Library for Light Water Reactors," RSIC-DLC-76, ORNL Radiation Shielding Information Center, Oak Ridge, TN, (1983).
5. J.F. Briesmeister, Editor, "MCNP - A General Monte Carlo N-Particle Transport Code, Version 4A," Los Alamos National Laboratory report LA-12625 (1993).
6. A. Haghghat, B.G. Petrovic, M. Mahgerefteh, "Estimation of Neutron Source Uncertainties in Pressure Vessel Fluence Calculations," *Trans. Am. Nucl. Soc.*, **69**, 459-461 (Nov. 1993).
7. A. Haghghat, et al., "Application of the Adjoint Function Methodology for Neutron Flux Determination," *Trans. Am. Nucl. Soc.*, **63**, 419-420 (June 1991).
8. J.C. Wagner, A. Haghghat, B.G. Petrovic, "Comparison of Monte Carlo and Synthesized 3-D Deterministic Models for Reactor Cavity Dosimetry Calculations," *Proc. Eighth Int. Conf Radiation Shielding*, Arlington TX (Apr. 1994).
9. M.L. Williams, C. Aboughantous, J.E. White, Q.R. Wright, F.B.K. Kam, "Transport Calculations of Neutron Transmission Through Steel Using ENDF/B-V, Revised ENDF/B-V, and ENDF/B-VI Iron Evaluations," NUREG/CR-5648, ORNL/TM-11686, Oak Ridge National Laboratory, (Apr. 1991).
10. B.G. Petrovic, A. Haghghat, "Effect of the Quadrature Order on the Accuracy of Fluence Calculations," *Trans. Am. Nucl. Soc.*, **68**, 477-479 (June 1993).
11. J.C. Wagner, E.L. Redmond II, S.P. Palmtag, J.S. Hendricks, "MCNP: Multigroup/Adjoint Capabilities," Los Alamos National Laboratory report, LA-12704 (1994).
12. "BUGLE-93: Coupled 47 Neutron, 20 Gamma-Ray Group Cross Section Library Derived from ENDF/B-VI for LWR Shielding and Pressure Vessel Dosimetry Applications," DLC-175, Oak Ridge National Laboratory, Radiation Shielding Information Center (1994).
13. H.L. Hanshaw, A. Haghghat, "Estimation of the Effects of Self-Shielding on Multigroup Reactor Vessel Fluence Calculations," *Trans. Am. Nucl. Soc.*, **71**, (1994).
14. R.W. Roussin, et. al., "VITAMIN-C: The CTR Processed Multigroup Cross Section Library for Neutronics Studies," Oak Ridge National Laboratory, ORNL-RSIC-37 (1980).

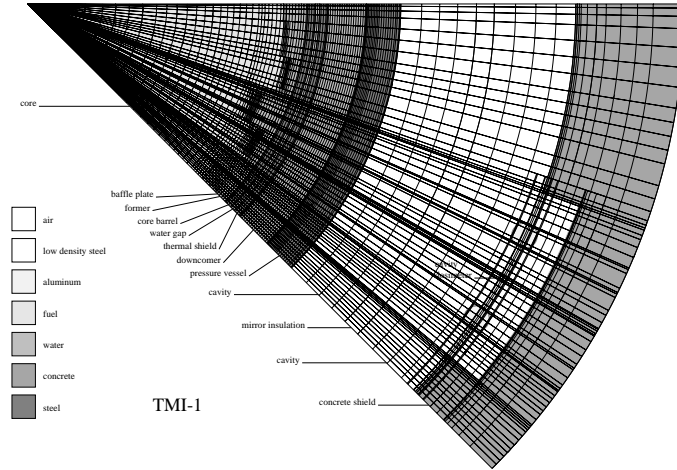


Fig. 1. Radial Cross-Section of DORT Model of TMI-1

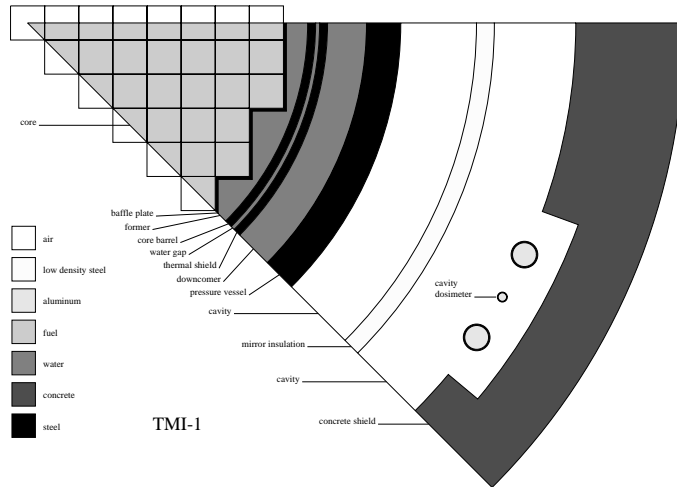


Fig. 2. Radial Cross-Section of MCNP Model for TMI-1

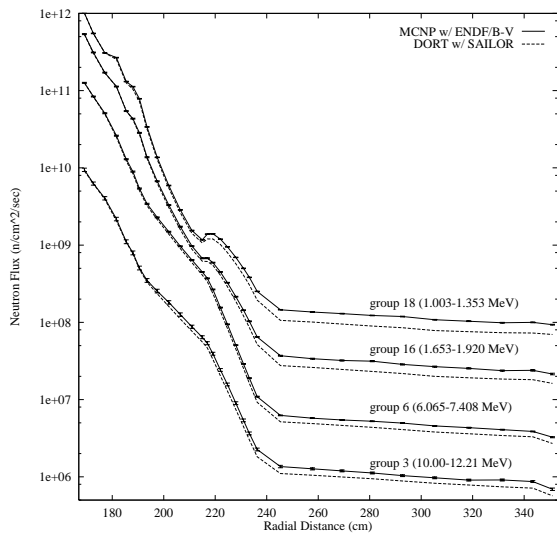


Fig. 3. Radial Flux Distributions for Groups 3, 6, 12, and 16

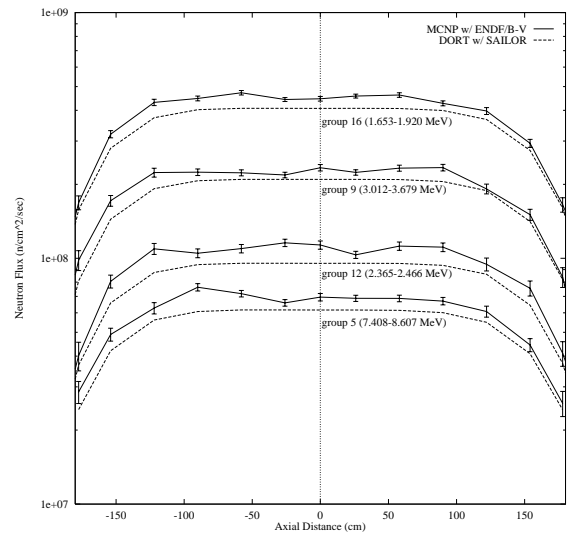


Fig. 4. Axial Flux Distributions for Groups 5, 9, 12, and 16

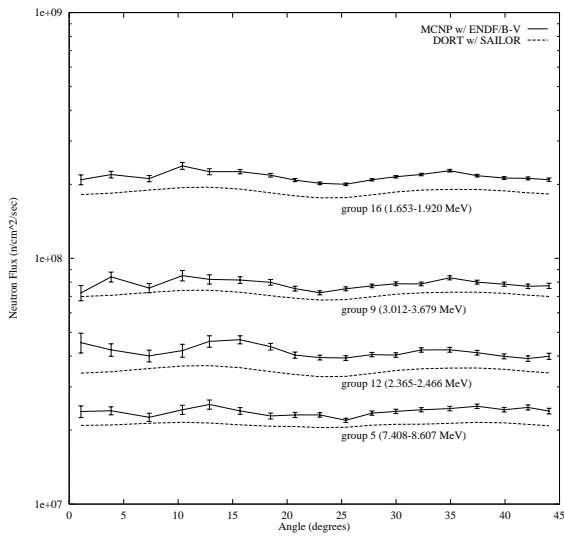


Fig. 5. Azimuthal Flux Distributions for Groups 5, 9, 12, and 16

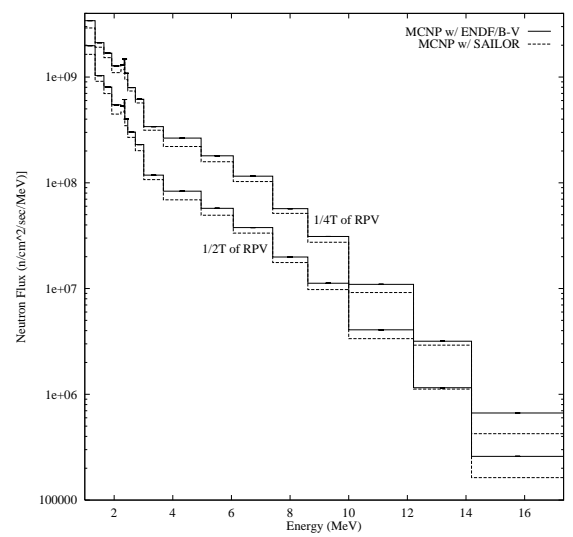


Fig. 6. Neutron Spectra at the $\frac{1}{4}T$ and $\frac{1}{2}T$ positions of the RPV

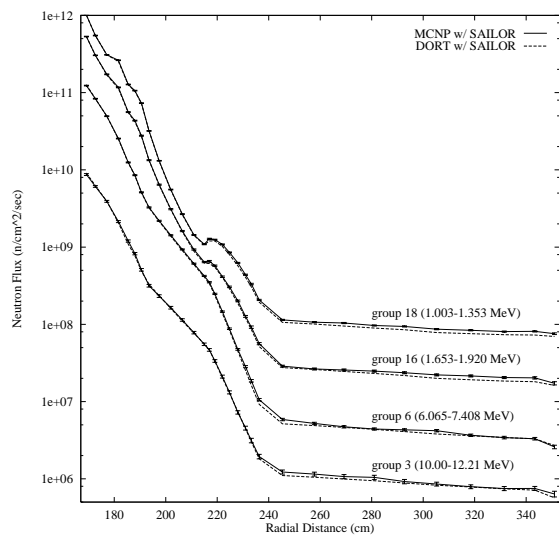


Fig. 7. Radial Flux Distributions for Groups 3, 6, 12, and 16

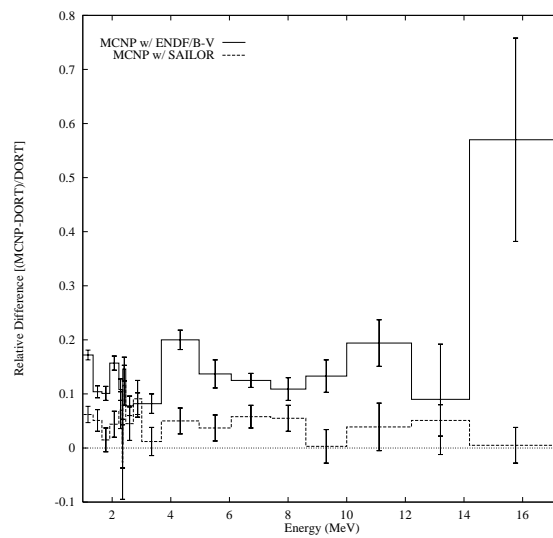


Fig. 8. Relative Difference in Neutron Spectra at the $\frac{1}{2}T$ position of the RPV

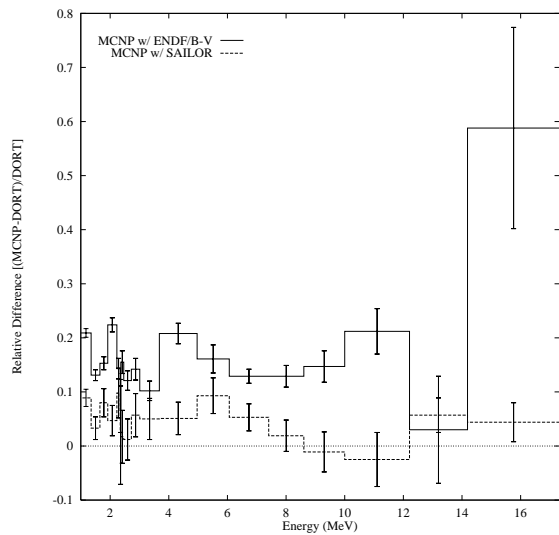


Fig. 9. Relative Difference in Neutron Spectra at the $\frac{1}{2}T$ position of the RPV

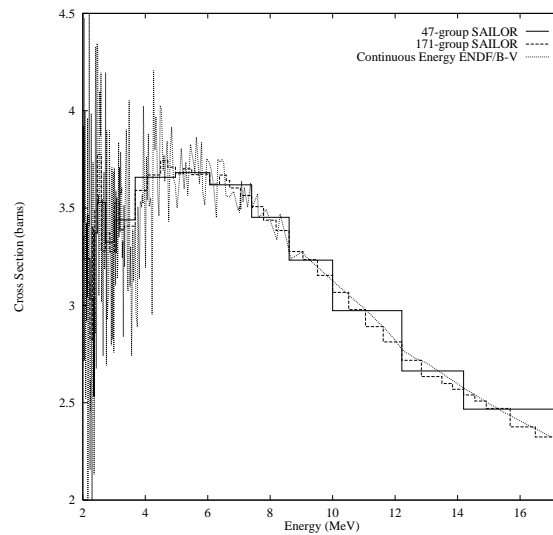


Fig. 10. Comparison of Representations of the Total Cross Section of Iron